

Preliminary Results of the Ground/Orbiter Lasercomm Demonstration Experiment between Table Mountain and the ETS-VI Satellite

K. E. Wilson, J. R. Lesh

Jet Propulsion Laboratory, California Institute of Technology

K. Araki, Y. Arimoto

Communications Research Laboratory, Tokyo Japan

The Ground/Orbiter Lasercomm Demonstration (GOLD) is an optical communications demonstration between the Japanese Engineering Test Satellite (ETS-VI) and an optical ground transmitting and receiving station at the Table Mountain Facility in Wrightwood California. Laser transmissions to the satellite are performed approximately four hours every third night when the satellite is at apogee above Table Mountain. The experiment required the coordination of resources at CRL, JPL, NASDA's Tsukuba tracking station and NASA's Deep Space Network at Goldstone, CA to generate and transmit real-time commands and receive telemetry from the ETS-VI. Transmissions to the ETS-VI began in November 1995 and are scheduled to last into the middle of January 1996 when the satellite is expected to be eclipsed by the Earth's shadow for a major part of its orbit. The eclipse is expected to last for about two months, and during this period there will be limited electrical power available on board the satellite. NASDA plans to restrict experiments with the ETS-VI satellite during this period, and no laser transmissions are planned. Post-eclipse experiments are currently being negotiated. GOLD is a joint NASA-CRL (Communications Research Laboratory) experiment that is being conducted by JPL in coordination with CRL and NASDA.

Keywords: GOLD, ETS-VI, LCE Lasercomm, Table Mountain Facility, Optical Communications

1. INTRODUCTION

The Ground/Orbiter Lasercomm Demonstration (GOLD) is a joint NASA/CRL (Communications Research Laboratory) optical communications experiment to evaluate 1-way and 2-way optical communications under a range of atmospheric conditions and to demonstrate optical ranging. The experiment's objectives are elaborated below.

Objectives

- Demonstrate 2-way spatial acquisition/tracking of laser beams with a spacecraft
- Accomplish 1-way and 2-way optical data transfer to a spacecraft and measure bit error rates
- Validate optical communications link performance prediction, tools
- Accumulate 10 elapsed hours of transmission/reception experience
- Compare downlink atmospheric transmission losses with similar data from the Table Mountain Facility's (TMF) Atmospheric Visibility Monitoring (AVM) observatory
- Demonstrate optical ranging to 10-m accuracy

GOLD experiments used the 0.6-m and 1.2-m telescopes located at NASA's TMF to communicate with the Japanese Engineering Test Satellite (ETS-VI). The experiment concept is depicted in figure 1.1. An Argon Ion laser coupled to the 0.6 meter telescope transmits a 1.024 Mbps Manchester-coded PN sequence to the spacecraft. The ETS-VI in turn uses its AlGaAs laser to transmit a similar PN sequence to the 1.2-m ground receiver located approximately 60-m from the transmitter site.

The ETS-VI was launched into orbit on August 28, 1994. Originally intended to be in a geo-stationary orbit above Japan, difficulty with one of its motors resulted in the satellite now being in a geo-transfer orbit. To make maximum use of the spacecraft's subsystems in its current orbit researchers at the Communications Research Laboratory encouraged both NASA and ESA experimenters to use the optical communications subsystem on board the ETS-VI. In response to this, NASDA relined the satellite's orbit to facilitate the use of the Laser Communications Equipment (LCE) by experimenters at JPL.

Yet, because the satellite's elliptical orbit takes the satellite through the Van Allen belts its power generation capabilities continued to degrade and its expected life reduced. Between mid-January and mid-March 1996 the satellite goes into a two-month-long eclipse. As of this writing, NASDA has continued to monitor the power generation capabilities of the satellite and has not yet made any commitments on post-eclipse experiments.

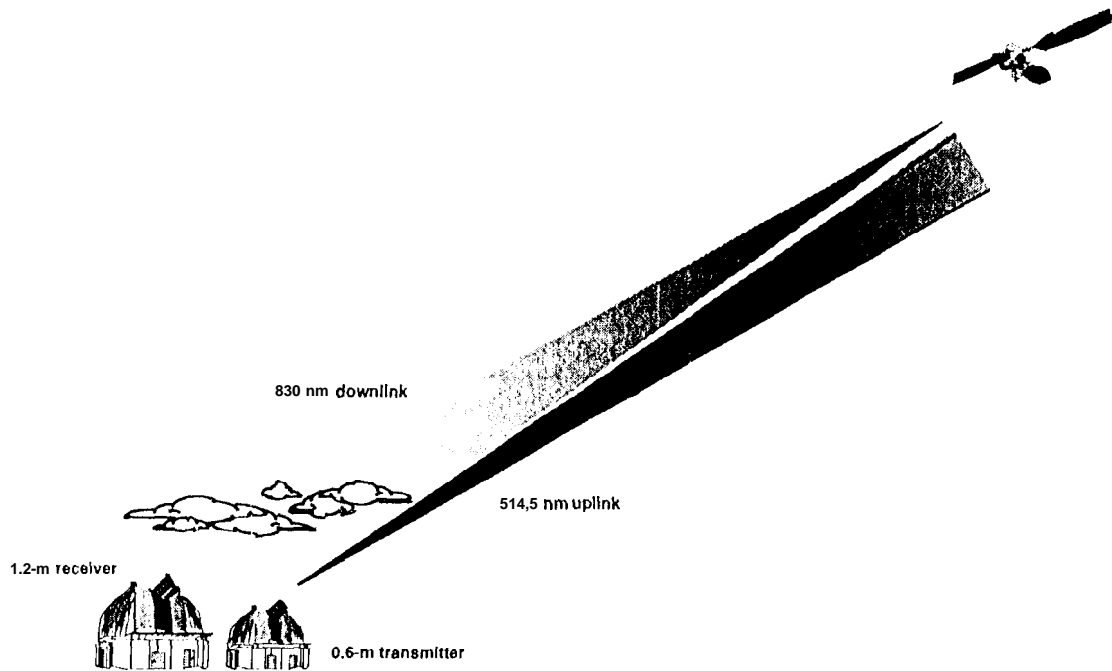


Figure 1.1.1: Conceptual drawing of GOLD. Transmitter at TMF uplinks 514.5 nm communications signal to ETS-VI spacecraft. Satellite downlinks 830 nm 1 Mbps signal,

This paper describes the work on GOLD part 1. The transmitter and receiver stations, the satellite predict generation process, and data link between TMF, NASDA and the CRI are discussed in Section 2. In Section 3 we describe the modifications to the satellite's trajectory that were made by the CRI team to enable the satellite to detect the uplink from and to retransmit an optical signal to TMF. Theoretical predictions and experiment results are presented in Section 4, and Conclusions and Acknowledgments are in Sections 5 and 6, respectively.

2. THE GOLD GROUND STATIONS

2.1.1 The Transmitter

The transmitter consisted of an Argon-ion laser coupled to the 0.6-m telescope at TMF. The telescope is located in building TM-12 at TMF, and its surveyed position is:

Longitude	117°40' 52.55"
Latitude	34°22' 53.49"
Altitude	2.286 km (7498.3')

The telescope was operated in the coude mode that allowed light to be coupled in to it from large high power lasers. The uplink laser was a prism tuned Coherent Innova-100 Ar-Ion that delivered a maximum of 14.5 Watts linearly polarizer laser light output power at 514.5 nm. Because the laser output was spatially multimode at maximum power, it was operated below maximum (typically 13 Watts) to achieve good beam quality. Coalignment of the laser beam with the telescope

axis was achieved by adjusting the position of the telescope's secondary mirror until the focus was brought to a position on the optical bench. At this setting the telescope's focal ratio was $f/41$, i.e., a focal length of 26.4 -m.

A schematic of the optical train is shown in figure 2.1.1.1. An electro-optic modulator was used to impress the uplink data stream on the optical carrier. The modulator consisted of four KD*P crystals and a polarizer. A data formatter - a Firebird 6000 bit error rate tester (BERT)- generated a 0 to 1 volt modulation pattern that was amplified to the modulator's half-wave voltage and applied to the crystals.

After modulation, the beam was incident on a concave/convex lens pair that set the beam divergence out of the telescope. This normally ranged from 20 urad to 40 urad. To mitigate the effects of atmospheric scintillation on the uplink beacon, the output beam was split into two equal parts using a beam-splitter. One beam was sent through a 25 cm optical delay line; a path length difference greater than the laser's 10 cm coherence length. Both beams were reflected from a high power dichroic beam-splitter and were brought to a focus at the iris located at the $f/41$ focus of the telescope. From there the beams diverged and were reflected by the third coude flat and into the telescope. The beams were arranged to be incident on opposite sides of the 0.6-m telescope's primary mirror, a distance greater than the size of an atmospheric coherence cell.

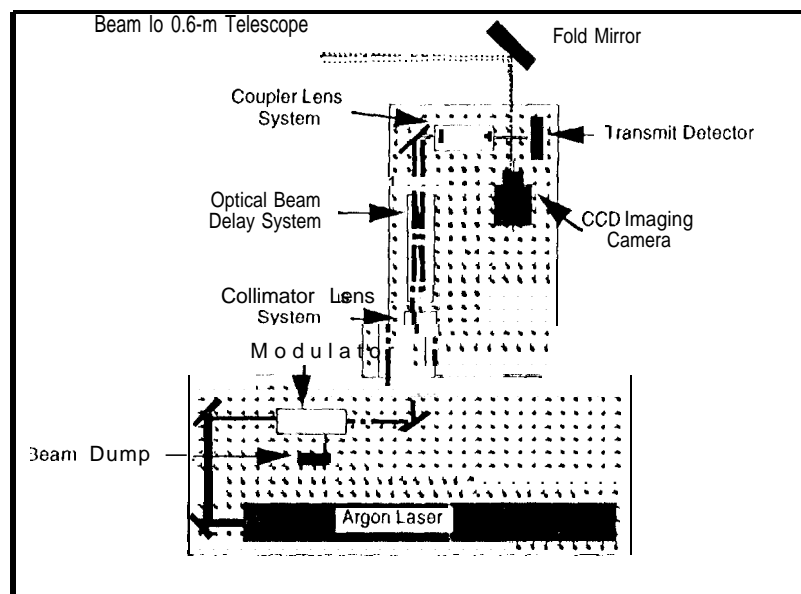


Figure 2.1.1.1: This schematic of optical train for GOLD experiment shows laser, the modulator, and the optical beam delay system used to provide "temporal and spatial diversity of the optical beams transmitted to the satellite. Also shown are the detector used to monitor the modulated wave form and the CCD camera used to image the satellite.

The CCD imaging camera was a Pulnix camera with image intensifier that enabled detection down to 10^{-6} lux. This camera enabled us to track the satellite around apogee where, depending on the phase angle of the solar panels, its brightness varied from that of a magnitude 12 to a magnitude 14 star. The avalanche photodiode (APD) transmitter detector monitored the modulation of the transmitted signal.

2.1.2, The Receiver

The receiver consisted of an optical detection package that weighed approximately 30 kg and a 1.2-m ($f/29.5$) telescope. The detection package was mounted to the telescope's bent Cassegrain focus, and consisted of two CCD cameras and a 3-mm diameter low-noise APD. See Figure 2.1.2.1. The cameras were a wide-field Cohu with image intensifier for satellite acquisition and tracking, and a Spectra Source CCD for making atmospheric seeing measurements. The detectors were colligned on a rigid optical bench assembly to ensure that the downlink transmission remained incident on both the tracking and communications detectors as the telescope tracked the satellite across the sky.

Satellite acquisition at the receiver station was accomplished using a series of steps. It began with calibrating the pointing direction of the narrow field-of view 1.2-m telescope with that of a wide field 0.4-m guiding telescope attached to the 1.2-m telescope's frame. Calibration was accomplished by first acquiring a bright star in the guiding telescope and then adjusting the telescope pointing direction until the star was observed in the 1.2-m telescope. The telescope was then moved to a star (not always a bright star) in the vicinity of the satellite - the blind point accuracy of the telescope depended on separation between the calibration star and the satellite positions- and the pointing offsets noted for calibration. Near apogee, the satellite brightness ranged from 12 to 14th magnitude. Because of the large dynamic range between the calibration stars 3rd to 5th magnitude and the satellite, a # 2 optical density filter was placed in an electronically-switched filter holder located in front of the tracking camera. The filter is placed in the optical beam during the calibration and is switched out for satellite acquisition.

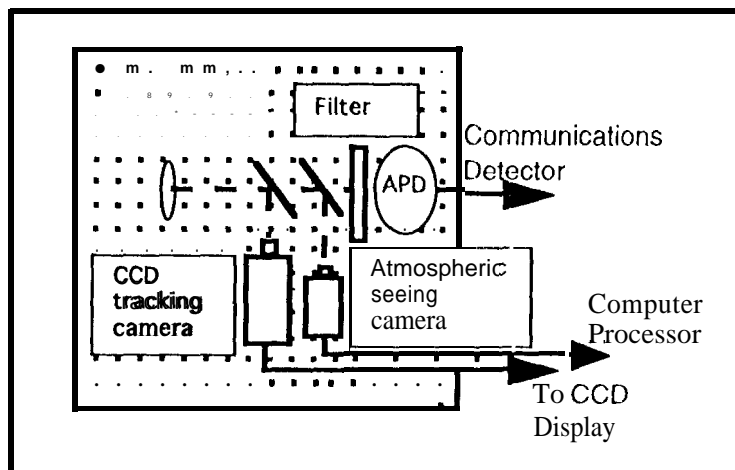


Figure 2.1.2.1: Schematic of optical receiver located at focus of 1.2-m telescope. CCDs detectors in the optical train track the satellite and measure atmospheric seeing. The APD detects the 1.024 Mbps optical downlink data stream.

Atmospheric seeing measurements provided essential data for evaluating the optical link performance. Theoretical models that incorporated scintillation effects into the link performance were compared with experimental. The seeing data were taken at 15 minute intervals to provide an accurate correlation between the atmospheric seeing and the observed uplink scintillation.

Downlink data recovery electronics started with the APD amplifier and signal conditioner. The satellite downlink data sequence was in one of three formats: 1.024 Mbps PN, real-time telemetry at 128 kbps with each bit repeated 8 times to produce a 1.024 Mbps data rate, and regenerated uplink square wave at 1 MHz. All data streams with the exception of the square wave modulation were Manchester coded. The amplified APD output was processed to provide both an analog and a digital output of the downlinked data stream. The digital output was bit-synchronized and stored on a data recorder for future processing. The analog data were displayed on a digital storage oscilloscope and segments stored on disk. A schematic of the receiver electronics is shown in Figure 2.1.2.2, and a segment of the PN downlinked analog data stream is shown in figure 2.1.2.3.

2.2 Satellite Predicts

The satellite predicts for the TMF telescopes were generated from a satellite osculating element set that was faxed to JPL from NASDA's Tsukuba Tracking Facility. Ephemeris files were generated at JPL for the transmitter and receiver telescopes, separately with OTSsets to account for the point-ahead angle. The files were electronically transmitted to TMF and were loaded into the telescope control program (TCP). The TCP used a spline fitting routine to interpolate between the ephemerides to generate a "smooth" telescope pointing file to track the ETS-VI satellite.

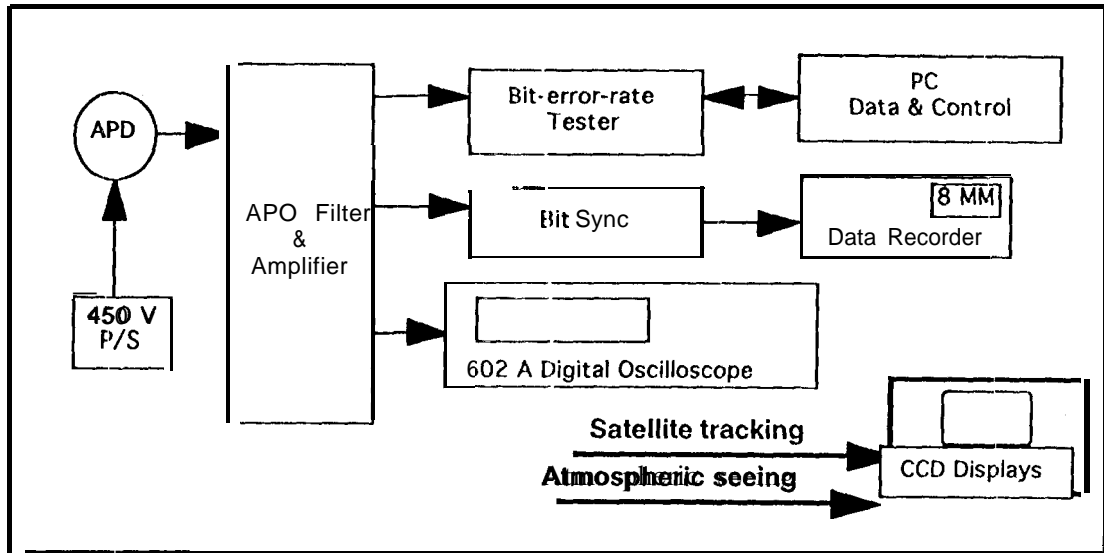


Figure 2.2.2: Schematic of downlink data recovery. The APD output is bit synchronized and recorded for later processing. The 602 A digital oscilloscope monitors the low-pass-filtered downlink signal for long-term signal amplitude variations,

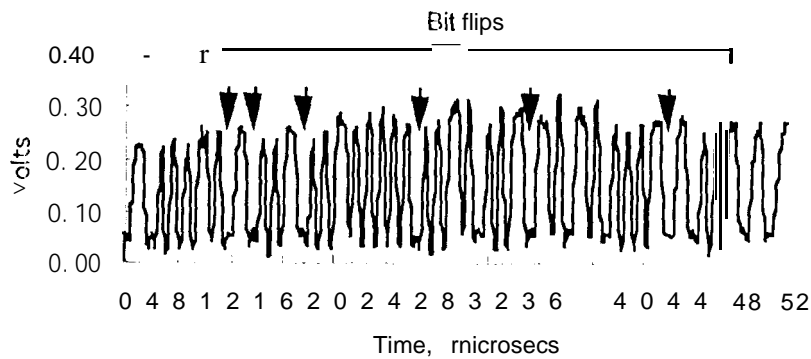


Figure 2.1.2.3: Sample of 1.024 Mbps Manchester-coded PN sequence downlink data-stream from LCE showing random bit flips. A few of these are indicated by arrows.

2.3 Data links

GOLD required the simultaneous real-time coordination of experimenters at the National Aeronautics and Space Development Agency (NASDA), at CRI, and the Deep Space Network (DSN) to accomplish the laser transmission from TMF. The command and data flow diagram is shown in Figure 2.3.1. In addition, prior to the installation of the aircraft avoidance radar, the Federal Aviation Administration's (FAA) Air Traffic Control Center in Palmdale provided aircraft avoidance assistance.

Commands to control the satellite's attitude during the experiment were generated at NASDA. CRI generated commands to control the LCE and sent these to NASDA. Both sets of commands were transmitted from NASDA to the 34-m 1) SS-27 antenna at Goldstone which then relayed them to the satellite.

The data link between CRI, JPL and TMF provided near-real-time feedback on the measured on-board laser communications equipment sensors to the experimenters at TMF. The delay between the spacecraft transmission and the TMF reception was approximately fifteen seconds. Spacecraft Attitude Control System (ACS) data was transmitted along with LCE data via S-band telemetry to 1) SS-27. The DSN transmitted these data to the NASDA Space Center at Tsukuba where they were demodulated, NASDA then transmitted the LCE data to CRI for processing. CRI, in turn transmitted an

ASCII data stream consisting of time, CCD level, QD level, spacecraft laser diode bias current, and coarse and fine tracking sensor errors via ISDN link to JPL. Because there are no ISDN (Integrated Services Digital Network) links to Wrightwood, a 56 kbps telephone link was used to transmit the data from JPL to TMF.

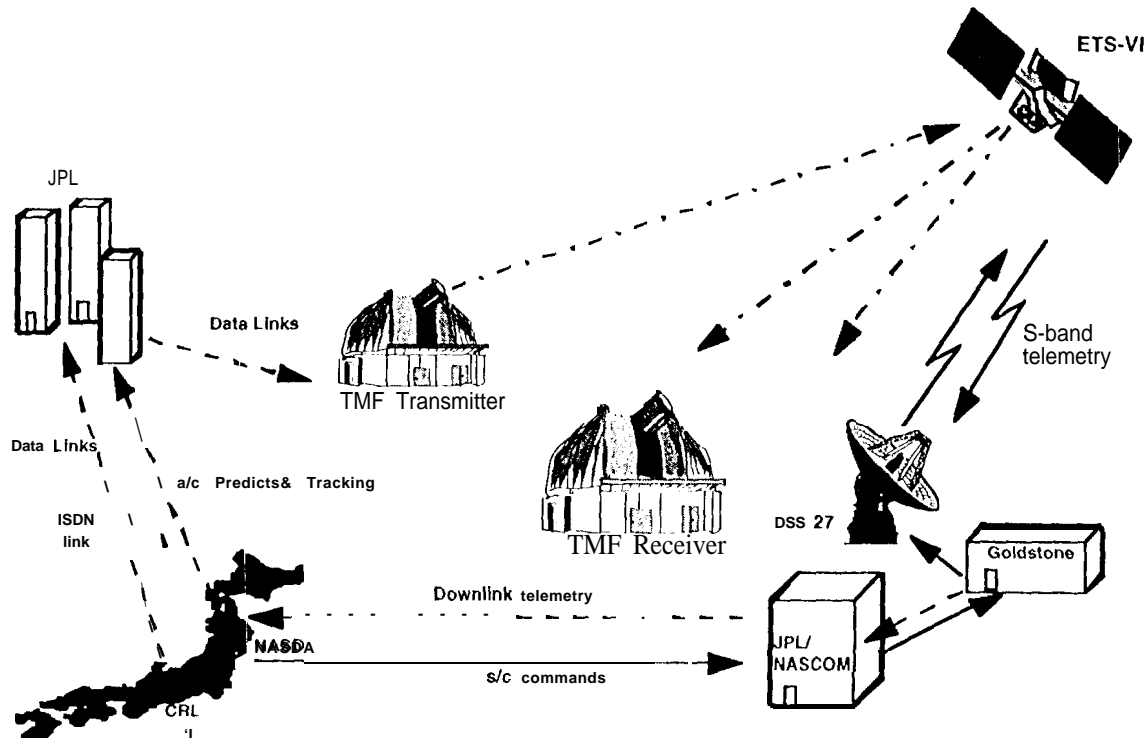


Figure 2.3.1: Real time coordination of several organizations is needed to accomplish the GOLD experiment. NASDA transfers commands to the DSN which uplinks them to the ETS-VI. The spacecraft attitude and LCE sensor status are down linked via S-band telemetry to Goldstone. The telemetry is demodulated by NASDA and forwarded to CRL for processing. During the optical uplink CRL transmits LCE sensor data to JPL and TMF.

3. ETS-VI TRAJECTORY MODIFICATIONS FOR GOLD

Because the ETS-VI was developed as a geo-stationary satellite, the LCE was designed with the pointing/tracking capabilities to support optical communications experiments from its location above Japan. The liquid apogee engine problem required that the operations scenario be revised to enable the satellite to support optical communications experiments. The satellite was transferred into a 3-day sub-recurrent orbit in November 1994, thereby enabling communication experiments to be performed from stations around the world. Figure 3.1.1 shows a three days prediction of the satellite's ground track from November 26, 1995. The figure also shows the section of the orbit where a combination of real-time satellite attitude control and LCE pointing (its pointing angle limited to ± 1 degree around its boresight direction) could allow an optical link between the satellite and TMF.

The angular pointing offsets between the ETS-VI and the TMF ground station were larger than those designed for a geo-stationary satellite link to Tokyo. To effect the laser communications experiments, NASDA had to re-program the onboard attitude control system (ACS) software to dynamically control the satellite's attitude bias. The satellite bias, however, was limited to the ± 2 degrees in roll and pitch that the JARH sensor's field-of-view allowed. The larger pointing offset between the satellite and TMF compared to the offsets for the Tokyo experiments meant that a series of experiments needed to be performed with the TMF station to calibrate the ACS and LCE biases for acquiring TMF.

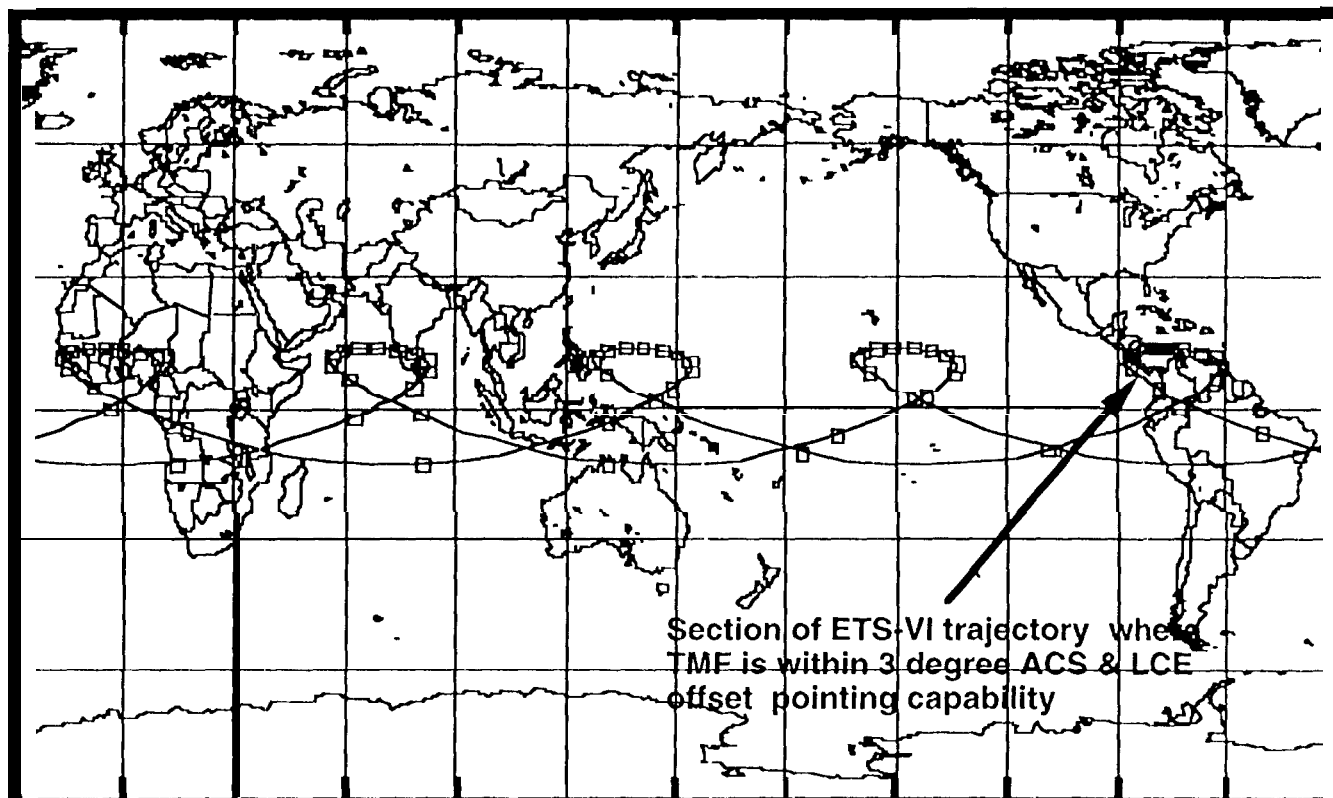


Figure 3.1.1: ETS-VI ground track showing the section (darkened area) where combined LCE and satellite ACS satellite pointing capabilities could support an optical communications experiment from TMF. The track covers November 26-29, 1995. The markers are one hour time spans

Figure 3.2 shows that the satellite pointing angle for TMF exceeded the limit of satellite attitude biasing control: the attitude bias angle needed to be greater than 2.5 degrees in order to point to the TMF ground station. The required pointing angle bias for GOLD was achieved by using the bias pointing capabilities of both the ACS and LCE as follows: one part was dynamically controlled by the ACS with a magnitude less than 2.0 degrees, and another was a fixed part shared by the LCE's pointing angle with its magnitude of 1.0 degree. As the figure shows, this approach allowed for approximately three hours of experiments from TMF. However, this window continued to decrease with time as the satellite's orbit configuration drifted. This is shown in Table 3.1, where based on the satellite's orbital configuration on October 3, 1995, the predicted duration of the satellite pass above the TMF ground station decreased by 26 minutes over the 18 passes between October 3 and November 23.

To maximize the pass duration from TMF while maintaining a viable experiment from CRI, NASA and CRI evaluated the effect of shifting the satellite's turn-around longitude (see figure 3.1) on the experiment duration from the two ground stations. The results are shown in Table 3.2 for several different orientations of the satellite's turn-around longitude. The table clearly shows that the pass duration above TMF continuously increases as the tracking azimuth angle at the turn-around point from CRI is increased from 150 degrees to 164 degrees. However, as the turn-around azimuth exceeds 160 degrees, the duration of the pass above CRI decreases rapidly. Based on these results the CRI and NASA implemented satellite orbit maneuvers that increased the satellite turn-around longitude to 160 degrees. These maneuvers were executed on November 25, 1995 and December 12, 1995, and they increased the passes at TMF by approximately one hour while maintaining the duration of the CRI pass.

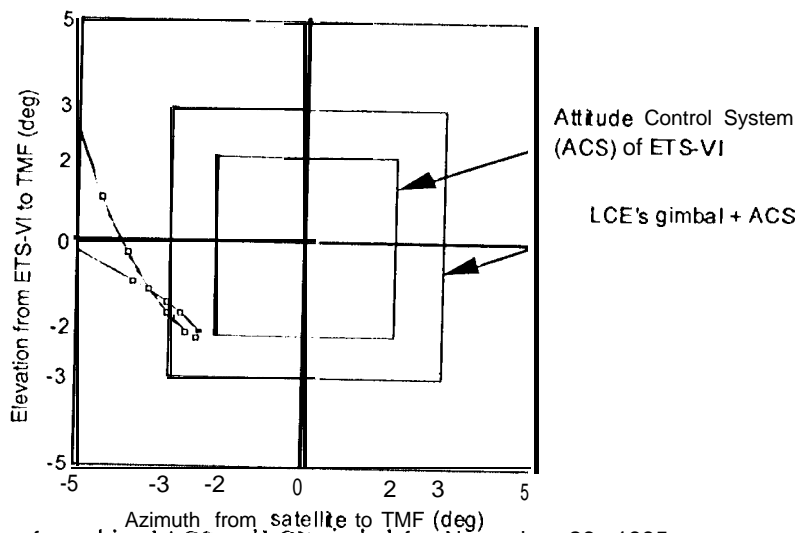


Figure 3.2: Plot of control region of combined ACS and LCE gimbal for November 26, 1995 pass over TMF, after the first orbit maneuver. Markers are separated by one hour, and trace shows (within the LCE gimbal + ACS area) approximately a five hour experiment window.

Table 3.1. Pass prediction from TMF based on 150 degree turn-around longitude on October 3, 1995

Start Time (UT)		End Time (UT)		Duration (Hours)
1995/10/03	13:21	1995/10/04	16:54	3:33
1995/10/06	13:11	1995/10/07	16:43	3:32
1995/10/09	13:01	1995/10/10	16:31	3:30
1995/10/12	12:52	1995/10/13	16:21	3:29
1995/10/15	12:42	1995/10/16	16:09	3:27
1995/10/18	12:32	1995/10/19	15:58	3:26
1995/10/21	12:23	1995/10/22	15:47	3:24
1995/10/24	12:13	1995/10/25	15:36	3:23
1995/10/27	12:03	1995/10/28	15:24	3:21
1995/10/30	11:54	1995/10/31	15:14	3:20
1995/11/02	11:44	1995/11/03	15:02	3:18
1995/11/05	11:34	1995/11/05	14:50	3:16
1995/11/08	11:25	1995/11/08	14:40	3:15
1995/11/11	11:15	1995/11/11	14:28	3:13
1995/11/14	11:05	1995/11/14	14:17	3:12
1995/11/17	10:56	1995/11/17	14:06	3:10
1995/11/20	10:46	1995/11/20	13:55	3:09
1995/11/23	10:36	1995/11/23	13:43	3:07

Table 3.2. Pass prediction of ETS-VI from TMF and CRI experimental site

Turn-around Longitude, degrees	150	152	158	160	162	164	152	158	160	162	164	
Start Time (UT)	Duration at TMF						Duration at CRI					
1995/11/26	10:26	3:06	3:21	4:34	4:53	5:14	5:32	3:58	3:48	3:27	2:59	2:28
1995/11/29	10:17	3:04	3:19	4:33	4:52	5:13	5:31	3:58	3:49	3:28	2:59	2:29
1995/12/02	10:07	3:03	3:18	4:32	4:51	5:12	5:30	3:58	3:50	3:29	3:00	2:31
1995/12/05	9:57	3:01	3:16	4:31	4:50	5:11	5:29	3:57	3:50	3:29	3:01	2:32
1995/12/08	9:48	3:00	3:15	4:30	4:49	5:10	5:28	3:56	3:50	3:30	3:02	2:33
1995/12/11	9:38	2:58	3:13	4:29	4:48	5:09	5:27	3:56	3:49	3:31	3:03	2:33
1995/12/14	9:28	2:57	3:12	4:28	4:47	5:08	5:26	3:55	3:48	3:31	3:03	2:34
1995/12/17	9:18	2:55	3:11	4:27	4:46	5:07	5:25	3:54	3:47	3:32	3:05	2:35
1995/12/20	9:09	2:53	3:09	4:25	4:45	5:06	5:24	3:54	3:47	3:33	3:06	2:36
1995/12/23	8:59	2:52	3:07	4:24	4:44	5:05	5:23	3:54	3:45	3:34	3:07	2:37
1995/12/26	8:49	2:50	3:06	4:23	4:42	5:04	5:22	3:53	3:45	3:34	3:07	2:39
1995/12/29	8:39	2:49	3:05	4:22	4:41	5:03	5:22	3:52	3:45	3:34	3:08	2:39
1996/01/01	8:30	2:47	3:03	4:21	4:40	5:02	5:21	3:52	3:44	3:36	3:09	2:40
1996/01/04	8:20	2:46	3:02	4:20	4:39	5:01	5:20	3:52	3:43	3:35	3:10	2:41
1996/01/07	8:10	2:45	3:00	4:18	4:38	5:00	5:19	3:51	3:43	3:35	3:10	2:42
1996/01/10	8:00	2:43	2:59	4:17	4:37	4:59	5:18	3:51	3:42	3:34	3:11	2:43
1996/01/13	7:51	2:42	2:58	4:16	4:36	4:58	5:18	3:50	3:41	3:34	3:12	2:43

4. EXPERIMENT RESULTS AND DATA ANALYSIS

There were twenty-six satellite passes over TMF (a satellite transmission pass was scheduled every third day) during the period October 30, 1995 to January 13, 1996. The passes were initially about 3 hours in duration; this was increased to about 5 hours after the November 25 satellite maneuver. Experiments on Thanksgiving, Christmas and New Years holidays were canceled to allow team members to be with their families. Approximately five of the passes were canceled due to weather, an additional one for a telescope scheduling conflict, and two more for unavoidable equipment anomalies. The first two operational passes were used to shake out the ground telescope systems and to learn how to coordinate remotely with the CRI satellite controllers. No signal detections were observed on those nights. On the 13 remaining passes, both uplink and downlink signal detections were accomplished.

Uplink signal detection was confirmed by monitoring the voltage levels on the spacecraft optical communication terminal's CCD and QD tracking detectors. Telemetry readings of these voltage levels were radio-transmitted to the ground, processed by CRI, and transmitted over communications lines to Table Mountain. These data were sampled at intervals of one second and the latency of the data upon arrival at TMF was about 15 seconds. During the operational periods, detailed logs were kept of the uplink transmitter site's configurations, conditions and any observed characteristics. These logs were later overlaid onto the data records to correlate status changes in the equipment with changes in the recorded uplink data signals.

Figure 4.1 shows such an overlay onto data collected on the January 4, 1996 pass. The bottom trace shows the (maximum output) level from the spacecraft's coarse-pointing-gimbal's CCD array tracker. The top trace shows the output voltage of the spacecraft fine-pointing-loop's QD. The fluctuations of these signals are due to a combination of things, most importantly the uplink atmospheric turbulence, but also signal level variations due to uplink beam pointing and spacecraft pointing errors. These data were sampled once per second and cover a span of about 1 hour and 40 minutes. The drop-out toward the right of the top segment is believed to be the result of a temporary bias build-up in the satellite pointing ephemeris predicts at the transmitter. The QD signal shows consistent limiting at the 4.3 volt saturation level. The CCD signal shows less-frequent transitions to its 5.2 volt saturation level. These data are being analyzed to determine the system's responses to the transmitted signal configurations.

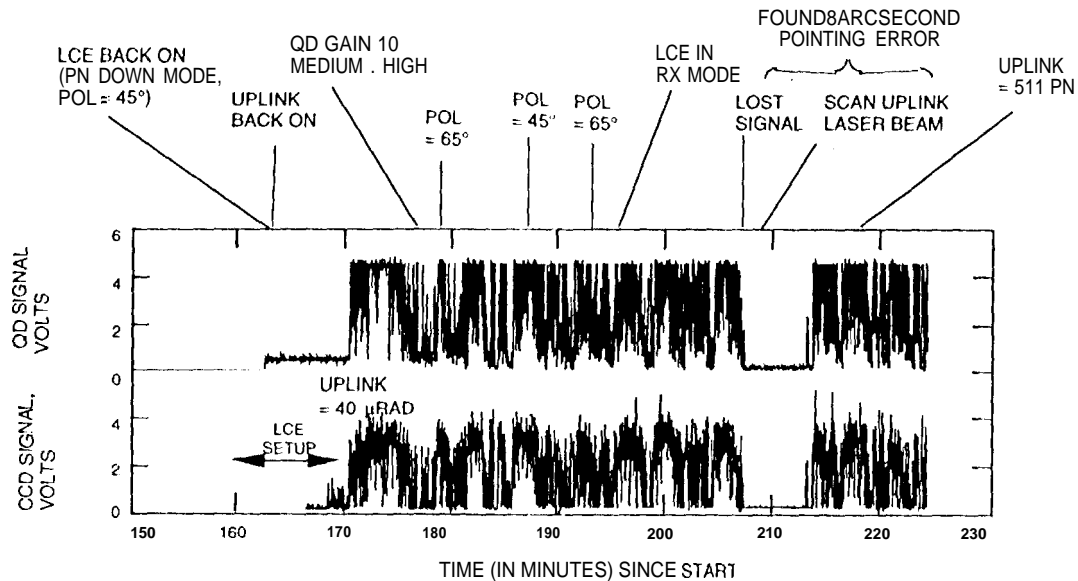


Figure 4.1: An annotated section of QD (top) and CCD (bottom) uplink signal levels for the January 4, 1996 satellite pass over TMF. Polarization sensitivity measurements and reacquisition of the uplink beam by the satellite after the transmitter telescope scan indicates that the satellite predicts were not very accurate for this pass. The uplink laser's beam divergence was 40 microradians. The annotation on the figure also shows the time at which the satellite mode was changed from PN to the regeneration or "RX " mode.

Before the operational passes of the program began in November 1995, we analyzed the expected uplink communications channel, consisting of the transmitting station parameters, the atmospheric and space propagation of the beam from the ground to the spacecraft at 40,000 km, and the spacecraft receiver parameters. This analysis led to a set of a-priori performance predicts for the signal strength at the spacecraft. To reduce the effects of uplink turbulence, we used a dual uplink beam approach where half of the power was placed into each of two spatially separated uplink beams. The beams combined in the far field to produce a full-power signal, but since the beams were in independent turbulence regions of the uplink telescope, there was averaging of the turbulence effects. The improvement due to this multi-beam averaging was included in the analysis.

Figure 4.2 shows a 100 minute segment of data collected from the spacecraft's QD on the morning of November 17. These data were fit to an appropriately-scaled log-normal distribution and the resulting distribution was compared with the theoretically estimated distribution generated a-priori. The results of this comparison are shown in Figure 4.3. The dotted curve shows the predicted log-normal distribution for a single beam uplink whereas the solid line shows the corresponding distribution for the dual-beam uplink. These curves clearly show the expected improvement due to the two-beam approach. The dashed curve is the log-normal distribution fitted to the experimental data taken on November 17. The comparison shows that the predicted distribution and the experimental one are extremely close. The difference in the distribution means is less than 1.6 dB.

Detection of the down link laser signal was also achieved on each of the 13 experimental nights at the 1.2 meter diameter receiving telescope. Detection was first confirmed by means of a video camera attached to the telescope's 0.4-m guide telescope. Data from this camera was videotaped during the passes. Downlink signals collected by the full 1.2-meter aperture were also detected using an avalanche photodiode detector and data from the resulting signals were recorded for analysis. A sample of the satellite telemetry data stream is given in figures 4.4. Included in this data are the measurements of the CCD, QD detector levels and BER measurements of the uplink.

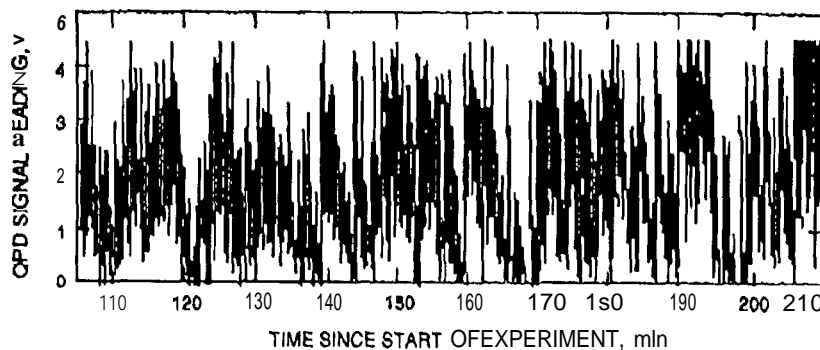


Figure 4.2: QD signal reading vs. time in minutes from start of the experiment (1 0:40 UT) on November 17, 1995.

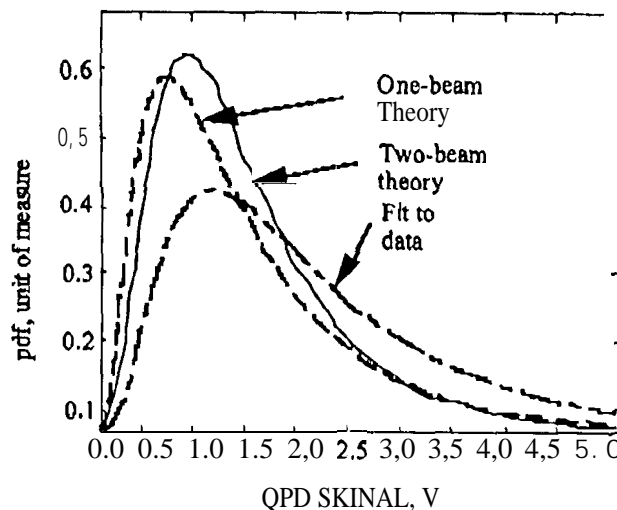


Figure 4.3: Theoretically predicted probability density functions for one and two beam uplinks are compared with the fitted curve from the GOLD uplink data. The theory, which does not include the effects of uplink pointing jitter, agrees reasonably with the experimental data, there is a 1.6 dB difference between the means of the measured and predicted distributions,

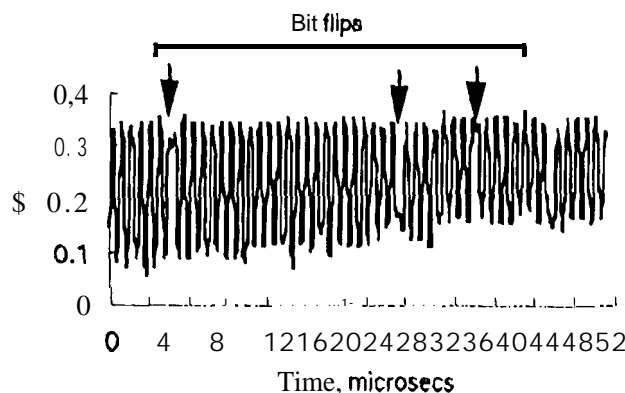


Figure 4.4: 128 kbps downlinked satellite telemetry. Data shows bit flips in multiples of eight consistent with the 8X repetition of the bit pattern,

5. CONCLUSIONS

GOLD was an **international** cooperative experiment that **demonstrated the** first optical signal regeneration between a satellite and an **optical** ground receiver, and the first low BER ground-to-space optical communications link to a satellite at **geo-**stationary distances. The thrust of the phase-1 experiment was to **measure and understand** the performance of the 2-way optical link under a variety of atmospheric attenuation and turbulence conditions. The data accumulated from this experiment will enable us to improve **our theoretical** models and to better define the performance of **the** technology for mission designers who are interested in optical communications for future missions. Satellite ranging using regeneration of an **uplinked** code is a time-tested approach in rf communications systems, A post-eclipse **GOLD opportunity will** allow us to investigate this approach at optical frequencies.

To date, we have amassed several **gigabytes** of data and video **tapes** of the optical links, along with measurements on the uplink scintillation. **These** data will be processed and the findings reported in future papers.

6. ACKNOWLEDGMENTS

The authors would like to acknowledge all of our fellow GOLD team members at the CRL, JPL, NASDA and the DSN. Their commitment and diligence *made it possible* to design procure and assemble the subsystems needed to convert the two TMF astronomical facilities into optical communications facilities in the short period of only four months,

The work described in this paper was performed by the Jet Propulsion Laboratory, California Institute of Technology, **under** contract with the National Aeronautics and Space Administration,